

Compressive acoustic sound speed profile estimation

Michael Bianco and Peter Gerstoft

Marine Physical Laboratory, Scripps Institution of Oceanography, La Jolla,
 California 92093-0238, USA
 mbianco@ucsd.edu, gerstoft@ucsd.edu

Abstract: Ocean acoustic sound speed profile (SSP) estimation requires the inversion of acoustic fields using limited observations. Compressive sensing (CS) asserts that certain underdetermined problems can be solved in high resolution, provided their solutions are sparse. Here, CS is used to estimate SSPs in a range-independent shallow ocean by inverting a non-linear acoustic propagation model. It is shown that SSPs can be estimated using CS to resolve fine-scale structure.

© 2016 Acoustical Society of America

[DRD]

Date Received: October 27, 2015 Date Accepted: February 2, 2016

1. Introduction

Inversion of ocean parameters using acoustic propagation models requires simultaneous optimization of water column sound speed profile (SSP) and sediment properties using limited observations. Such inverse problems are ill-posed, and require regularization to ensure physically realistic solutions.¹ The water column SSP estimation problem has been regularized traditionally by minimizing the energy of the solution to a least-squares cost function, which requires undersampling of complex SSP structure or explaining the structure using few shape functions.²⁻⁴ This reduction in resolution causes SSP uncertainty, especially when internal waves or currents generate strong, temporally varying SSP anomalies.⁵⁻⁷ This uncertainty can severely effect the accuracy of inversion for other parameters.^{6,7}

We show that SSPs in range-independent shallow ocean environments can be resolved using compressive sensing^{8,9} (CS). CS asserts that parameters can be recovered robustly for certain highly underdetermined linear problems via sparse regularization of a least-squares cost function, provided that the solutions are sparse, i.e., few non-zero parameters (out of many) explain the observations. Recent applications of CS in ocean acoustics have demonstrated performance improvements to coherent passive fathometry¹⁰ and beamforming¹¹⁻¹³ under sparsity assumptions. Here, the inversion for ocean acoustic SSPs is formulated as an underdetermined linear problem where SSP perturbations are parameterized in a sparse domain using shape functions.

Pressure observations from a vertical line array (VLA) of hydrophones in a shallow ocean are forward-modeled using normal modes. The non-linear response of the forward model to SSP is linearized using a first order Taylor expansion. The linearized sensitivities of few observations are calculated for many shape functions, which parameterize SSPs in a sparse domain. Thus, SSP estimation is expressed as an underdetermined linear problem and solved using convex optimization of a least squares cost function with an ℓ_1 sparsity constraint.^{8,9}

2. Compressive estimation of water column SSP

A K -point discretized ocean SSP, $\mathbf{c}(\mathbf{x}) \in \mathbb{R}^K$, is modeled as

$$\mathbf{c}(\mathbf{x}) = \mathbf{c}_0 + \mathbf{Q}\mathbf{x}, \quad (1)$$

where $\mathbf{c}_0 \in \mathbb{R}^K$ is a reference SSP (e.g., derived from historical statistics or CTD casts), $\mathbf{Q} = [\mathbf{q}_1, \dots, \mathbf{q}_N] \in \mathbb{R}^{K \times N}$ is a dictionary of N unique shape functions \mathbf{q}_n discretized into K points, and $\mathbf{x} \in \mathbb{R}^N$ is the dictionary coefficient vector. The SSP is modeled by shape functions¹ that describe SSP perturbations with few non-zero coefficients in \mathbf{x} . SSP perturbations that are isolated to specific depths of the water column are here modeled using half-sinusoidal shape functions. Larger SSP variation is modeled using EOFs.^{2,5,7}

The pressure $\mathbf{p}_{obs} \in \mathbb{C}^M$ received at an M element VLA is modeled as

$$\mathbf{p}_{obs} = \mathbf{g}(\mathbf{x}) + \mathbf{n}, \quad (2)$$

where $\mathbf{g}(\mathbf{x}) \in \mathbb{C}^M$ is the normal mode propagation given $\mathbf{c}(\mathbf{x})$ and $\mathbf{n} \in \mathbb{C}^M$ is Gaussian white noise. Here, the source is known and included in the $\mathbf{g}(\mathbf{x})$ term.

Assuming the perturbations to the reference SSP are small, the non-linear response of $\mathbf{g}(\mathbf{x})$ to SSP perturbations is linearized using the first order Taylor expansion

$$\mathbf{g}(\mathbf{x}) \approx \mathbf{g}(0) + \frac{\partial \mathbf{g}(\mathbf{x})}{\partial \mathbf{x}} \Big|_{\mathbf{x}=0} \mathbf{x} = \mathbf{g}(0) + \mathbf{D}\mathbf{x}. \tag{3}$$

The matrix $\mathbf{D} = [\mathbf{d}_1, \dots, \mathbf{d}_N] \in \mathbb{C}^{M \times N}$ contains the derivatives of the M pressure observations relative to the N shape functions in \mathbf{Q} . The columns \mathbf{d}_n are calculated using two-sided finite differences, by perturbing the reference profile by a fraction of \mathbf{q}_n .

Provided the columns of \mathbf{D} are sufficiently incoherent, a sparse estimate of \mathbf{x} is found using ℓ_1 -norm convex optimization.^{8,9} The sparse solution to Eq. (2) is formulated as

$$\hat{\mathbf{x}}_{\ell_1}(\mu) = \underset{\mathbf{x} \in \mathbb{R}^N}{\operatorname{argmin}} \left\| \frac{\mathbf{g}(0) + \mathbf{D}\mathbf{x}}{|\mathbf{p}_{obs}|} - \tilde{\mathbf{p}}_{obs} \right\|_2^2 + \mu \|\mathbf{x}\|_1, \tag{4}$$

where (assuming a signal is present) Eq. (2) is scaled by $|\mathbf{p}_{obs}|$ as

$$\tilde{\mathbf{p}}_{obs} = \frac{\mathbf{p}_{obs}}{|\mathbf{p}_{obs}|} = \frac{\mathbf{g}(0) + \mathbf{D}\mathbf{x} + \mathbf{n}}{|\mathbf{p}_{obs}|}, \tag{5}$$

$\hat{\mathbf{x}}_{\ell_1}$ is the sparse estimate of the SSP perturbation coefficients, and μ is the regularization parameter which controls the relative importance of sparsity (ℓ_1 -norm regularization) and measurement fit (ℓ_2 -norm). Equation (2) is scaled to improve numerical stability by reducing the difference in magnitude between the ℓ_1 -norm of \mathbf{x} and the ℓ_2 cost function.

The sparse solution $\hat{\mathbf{x}}_{\ell_1}$ selects the coefficients in \mathbf{x} that best explain the observations, but their values are biased.¹⁴ The coefficients are optimized using least-squares criteria by solving the overdetermined problem^{12,13}

$$\hat{\mathbf{x}}_{CS} = \mathbf{D}_A^+ [\mathbf{p}_{obs} - \mathbf{g}(0)], \tag{6}$$

where \mathbf{D}_A contains only the active columns of \mathbf{D} , corresponding to non-zero elements in $\hat{\mathbf{x}}_{\ell_1}$, and \mathbf{D}_A^+ is its Moore-Penrose pseudoinverse. Here, $\hat{\mathbf{x}}_{CS}$ is the optimal compressive sensing solution to Eq. (2).

The non-sparse (minimum energy) estimate $\hat{\mathbf{x}}_{\ell_2}$ of \mathbf{x} is written as

$$\hat{\mathbf{x}}_{\ell_2}(\mu) = \underset{\mathbf{x} \in \mathbb{R}^N}{\operatorname{argmin}} \left\| \frac{\mathbf{g}(0) + \mathbf{D}\mathbf{x}}{|\mathbf{p}_{obs}|} - \tilde{\mathbf{p}}_{obs} \right\|_2^2 + \lambda \|\mathbf{x}\|_2^2, \tag{7}$$

where λ controls the relative importance of solution energy (ℓ_2 -norm regularization) and measurement fit (ℓ_2 -norm).

3. Simulation and results

The acoustic field in a 160 m constant-depth ocean was simulated using the Kraken normal mode model.¹⁵ The field, generated by a 100 Hz acoustic source at 30 m depth, was sampled at 2 km range by $M=10$ evenly spaced VLA elements spanning 10 to 150 m depth. The reference SSP was the mean SSP from the SWellEx-96 experiment. The bottom sound speed was 1800 m/s, density 2.0 g/cm³, and attenuation 0.1 dB/λ. A diagram of the environment is shown in Fig. 1(a).

The sparse problems were solved using the CVX toolbox, which specifies and solves convex optimization problems.¹⁶ Sparsity of $\hat{\mathbf{x}}_{\ell_1}$, Eq. (4), was enhanced using reweighted ℓ_1 -norm minimization method; for details see Refs. 12 and 17. For comparison, the minimum energy estimate $\hat{\mathbf{x}}_{\ell_2}$ of the parameters, Eq. (7), was solved with $\lambda = 5 \times 10^{-5}$.

3.1 Compressive estimation of half-sinusoidal SSP perturbations

To simulate SSP anomalies confined to narrow depth ranges, two half-sinusoidal perturbations [Fig. 1(b)] were added to the reference SSP at depths of 63.3 and 126.7 m with magnitudes of ± 2 m/s and 20 m widths. Equation (3) was formulated with \mathbf{Q} containing $N=100$ half-sinusoid shape functions having the same widths as the perturbations.

Figures 2(a) and 2(b) shows the sparse solution $\hat{\mathbf{x}}_{CS}$, Eq. (6) after solving Eqs. (4) and (5), for the half-sinusoidal perturbations with 30 dB SNR for $\mu = 5 \times 10^{-4}$. It can be seen that for one realization of Gaussian white noise, the sparse magnitudes

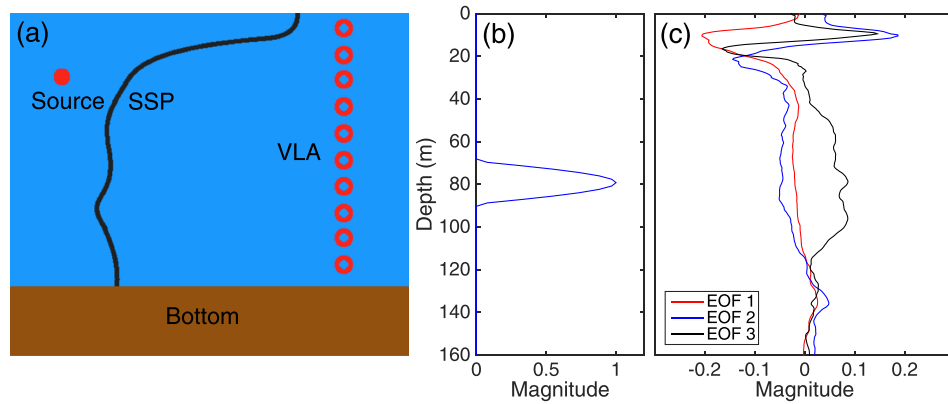


Fig. 1. (Color online) (a) Ocean environment and measurement configuration. (b) Half-sinusoid shape function. (c) First three EOFs derived from the SWellEx-96 data.

and locations of the perturbations were estimated accurately. With 10 observations and 100 potential shape functions, this problem was underdetermined by a factor of 10 and CS still gave an accurate result. The minimum energy solution \hat{x}_{ℓ_2} , Eq. (7), shown in Figs. 2(c) and 2(d), did not provide the true parameters. Instead the solution was non-sparse, having many small perturbations.

3.2 Compressive estimation of SSP using EOFs

A set of EOFs was calculated using 26 CTD casts spanning depths ≥ 160 m from the SWellEx-96 experiment, resulting in a dictionary \mathbf{Q} with $N=26$ EOFs. The first three EOFs are shown in Fig. 1(c). Synthetic SSPs and SWellEx-96 profiles were estimated using CS.

The robustness of the CS EOF inversion was tested by finding sparse estimates \hat{x}_{CS} for 1000 synthetic SSPs, having randomly selected active EOF components with coefficients of ± 6 m/s. The active EOF components were selected randomly from a half-Gaussian distribution, with the peak located at the first EOF, to simulate the relative importance of the EOFs. Each of the synthetic SSPs were compressively inverted without observation noise with $\mu = 5 \times 10^{-5}$ (corresponding to three sparse EOF

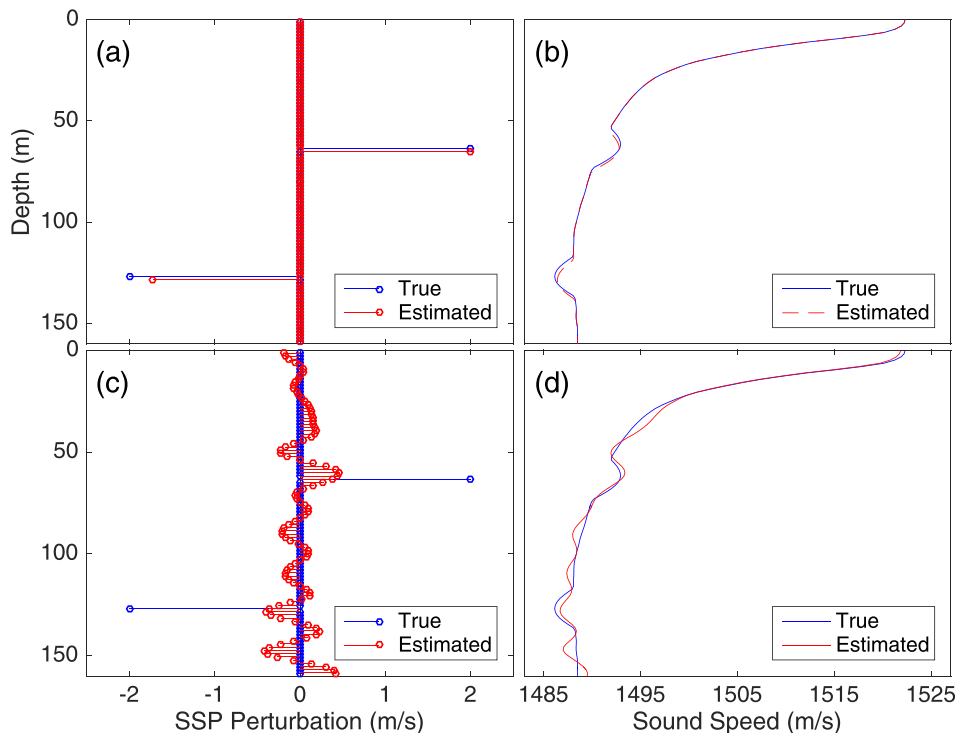


Fig. 2. (Color online) Sparse \hat{x}_{CS} [(a) and (b)] and minimum energy \hat{x}_{ℓ_2} [(c) and (d)] estimates for half-sinusoidal ocean SSP perturbations from noisy observations (SNR = 30 dB). [(a) and (c)] Depth and magnitude of perturbations, and [(b) and (d)] the corresponding SSPs.

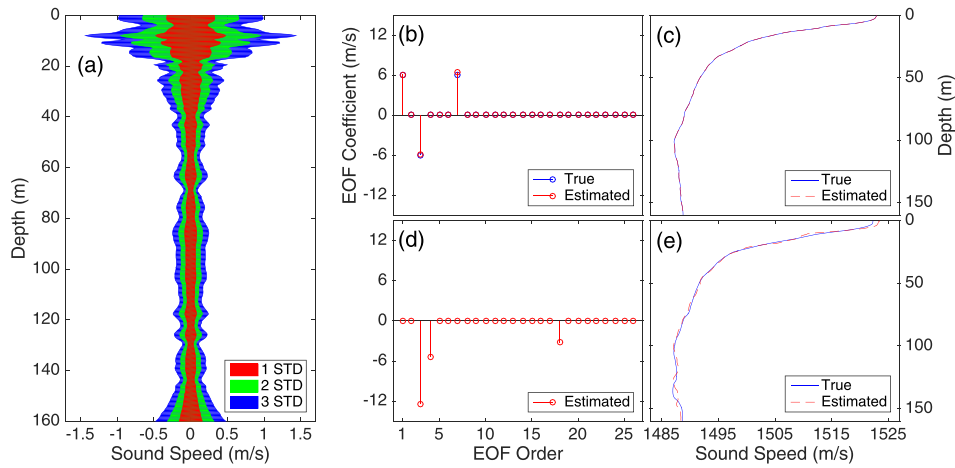


Fig. 3. (Color online) (a) SSP estimation error versus depth of the sparse solution \hat{x}_{CS} (without noise) for 1000 randomly generated synthetic SSPs with three EOF components. For one randomly generated SSP, \hat{x}_{CS} estimate (b) of the EOF coefficients and (c) the corresponding SSP. For one SWellEx-96 SSP, \hat{x}_{CS} estimate for (d) EOF coefficients and (e) corresponding SSP.

coefficients for most cases). The SSP estimation error [standard deviation (STD)] versus depth in Fig. 3(a) shows that SSP error increases toward shallow depths. This is likely due to downward refraction of the acoustic waves by the warmer surface water, which makes the inversion insensitive to near-surface variability. For deeper SSP variability, 1 STD of error is within ± 0.2 m/s. In Figs. 3(b) and 3(c) a CS EOF inversion result is shown for one random trial. Considering a SSP from the SWellEx-96 experiment, Figs. 3(d) and 3(e) shows CS inversion of three EOF components with $\mu = 1.5 \times 10^{-4}$.

Figures 4(a) and 4(b) shows the CS estimation of the three EOF SSPs used in Fig. 3 with a 30 dB SNR for $\mu = 2 \times 10^{-4}$ (μ increases due to noise). With one realization of Gaussian white noise, the EOF components are estimated. As shown in Figs. 4(c) and 4(d) the \hat{x}_{ℓ_2} solution was non-sparse and provided inaccurate estimates of the true (sparse) parameters.

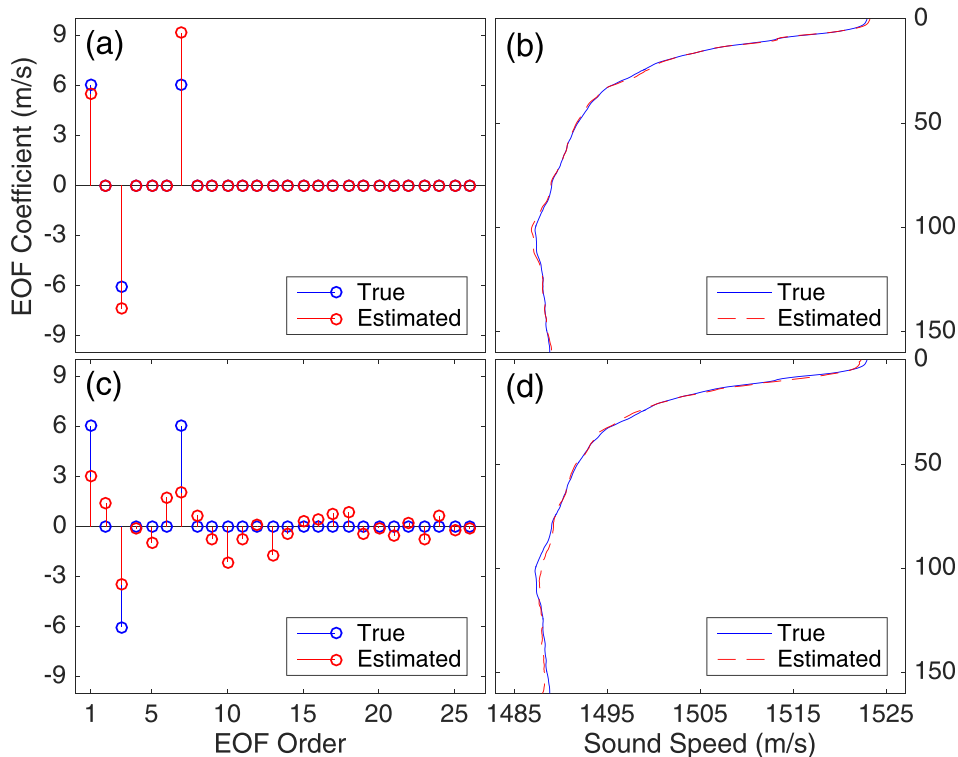


Fig. 4. (Color online) Sparse \hat{x}_{CS} [(a) and (b)] and minimum energy \hat{x}_{ℓ_2} [(c) and (d)] estimates of three SSP EOF coefficients from noisy observations (SNR = 30 dB). [(a) and (c)] EOF coefficients and [(b) and (d)] the corresponding SSPs.

4. Conclusion

A method for compressive inversion of ocean acoustic SSPs was developed and demonstrated. With medium SNR, *a priori* knowledge of the ocean sound speed statistics, and a dictionary of shape functions that sparsely represent the SSPs, fine-scale SSP structure is well estimated using CS. Robust recovery of sparse SSP perturbations was shown using dictionaries containing either half-sinusoidal shape functions or EOFs.

Acknowledgments

This work was supported by the Office of Naval Research, Grant No. N00014-11-1-0439.

References and links

- ¹P. Gerstoft, "Inversion of acoustic data using a combination of genetic algorithms and the Gauss-Newton approach," *J. Acoust. Soc. Am.* **97**, 2181–2190 (1995).
- ²B. A. Tan, P. Gerstoft, C. Yardim, and W. S. Hodgkiss, "Broadband synthetic aperture geoacoustic inversion," *J. Acoust. Soc. Am.* **134**, 312–322 (2013).
- ³C. Park, W. Seong, P. Gerstoft, and W. S. Hodgkiss, "Geoacoustic inversion using backpropagation," *IEEE J. Ocean. Eng.* **35**, 722–731 (2010).
- ⁴M. I. Taroudakis and J. S. Papadakis, "A modal inversion scheme for ocean acoustic tomography," *J. Comp. Acoust.* **1**, 395–421 (1993).
- ⁵Y. T. Lin, C. F. Chen, and J. F. Lynch, "An equivalent transform method for evaluating the effect of water-column mismatch on geoacoustic inversion," *IEEE J. Ocean. Eng.* **31**, 284–298 (2006).
- ⁶M. Siderius, P. L. Nielsen, J. Sellschopp, M. Snellen, and D. Simons, "Experimental study of geoacoustic inversion uncertainty due to ocean sound-speed fluctuations," *J. Acoust. Soc. Am.* **110**, 769–781 (2001).
- ⁷C. F. Huang, P. Gerstoft, and W. S. Hodgkiss, "Effect of ocean sound speed uncertainty on matched-field geoacoustic inversion," *J. Acoust. Soc. Am.* **123**, EL162–EL168 (2008).
- ⁸E. Candés, "Compressive sampling," in *Proceedings of the International Congress of Mathematicians* (2006), Vol. 3, pp. 1433–1452.
- ⁹M. Elad, *Sparse and Redundant Representations* (Springer, New York, 2010), pp. 1–376.
- ¹⁰C. Yardim, P. Gerstoft, W. S. Hodgkiss, and J. Traer, "Compressive geoacoustic inversion using ambient noise," *J. Acoust. Soc. Am.* **135**, 1245–1255 (2014).
- ¹¹G. Edelmann and C. Gaumont, "Beamforming using compressive sensing," *J. Acoust. Soc. Am.* **130**, EL232–EL237 (2011).
- ¹²A. Xenaki, P. Gerstoft, and K. Mosegaard, "Compressive beamforming," *J. Acoust. Soc. Am.* **136**, 260–271 (2014).
- ¹³P. Gerstoft, A. Xenaki, and C. F. Mecklenbräuker, "Multiple and single snapshot compressive beamforming," *J. Acoust. Soc. Am.* **138**, 2003–2014 (2015).
- ¹⁴M. A. Figueiredo, R. D. Nowak, and S. J. Wright, "Gradient projection for sparse reconstruction: Application to compressed sensing and other inverse problems," *IEEE J. Sel. Topics Sign. Process.* **1**, 586–597 (2007).
- ¹⁵M. B. Porter, "The KRAKEN normal mode program," Report No. NRL/MR/5120-92-6920, Naval Research Laboratory, Washington, D.C. (1992).
- ¹⁶M. Grant and S. Boyd, "CVX: Matlab software for disciplined convex programming, version 2.1," <http://cvxr.com/cvx> (Last viewed October 20, 2015).
- ¹⁷E. J. Candés, M. B. Wakin, and S. P. Boyd, "Enhancing sparsity by reweighted ℓ_1 minimization," *J. Fourier Anal. Appl.* **14**, 877–905 (2008).